H_2-driven xylitol production in *Cupriavidus necator* H16

Tytti Jämsä[1,*] ID, Nico J. Claassens[2] ID, Laura Salusjärvi[1] ID, Antti Nyyssölä[1] ID

Abstract

Background: Biocatalysis offers a potentially greener alternative to chemical processes. For biocatalytic systems requiring cofactor recycling, hydrogen emerges as an attractive reducing agent. Hydrogen is attractive because all the electrons can be fully transferred to the product, and it can be efficiently produced from water using renewable electricity. In this article, resting cells of *Cupriavidus necator* H16 harboring a NAD-dependent hydrogenase were employed for cofactor recycling to reduce D-xylose to xylitol, a commonly used sweetener. To enable this bioconversion, D-xylose reductase from *Scheffersomyces stipitis* was heterologously expressed in *C. necator*.

Results: D-xylose reductase was successfully expressed in *C. necator*, enabling almost complete bioconversion of 30 g/L of D-xylose into xylitol. It was found that over 90% of the energy and protons derived from hydrogen were spent for the bioconversion, demonstrating the efficiency of the system. The highest xylitol productivity reached was 0.7 g L^{-1} h^{-1}. Additionally, the same chassis efficiently produced L-arabitol and D-ribitol from L-arabinose and D-ribose, respectively.

Conclusions: This study highlights the efficient utilization of renewable hydrogen as a reducing agent to power cofactor recycling. Hydrogen-oxidizing bacteria, such as *C. necator*, can be promising hosts for performing hydrogen-driven biocatalysis.

Affiliations

[1] VTT Technical Research Centre of Finland Ltd., Tekniikantie 21, 02150 Espoo, Finland

[2] Laboratory of Microbiology, Wageningen University, Stippeneng 4, 6708WE Wageningen, the Netherlands

*Corresponding author E-mail address: tytti.jamsa@vtt.fi

Keywords

Biotransformation, cofactor recycling, cofactor regeneration, *Ralstonia eutropha*, *Cupriavidus necator*, hydrogen-oxidizing bacteria

Background

Biocatalysis is increasingly applied across different industries due to its efficiency and environmental benefits compared to chemical transformations. Biocatalysis using oxidoreductases often requires cofactors, such as nicotinamide nucleotides NADH and NADPH, but their stoichiometric addition to reaction mixtures is not economically feasible (1). Therefore, cofactor recycling systems are required. Traditionally cofactor recycling of NAD(P)H is performed using sacrificial substrates, such as glucose and formate, which are oxidized during the biocatalysis, while the cofactor is regenerated to its reduced form (2). This is not carbon-efficient, since D-gluconolactone and carbon dioxide (CO_2) are formed as by-products from glucose and formate, respectively. Specifically for the by-product D-gluconolactone, a substantial number of energy-rich electrons are wasted. In addition, glucose is produced by agriculture, which can decrease the overall sustainability of the production process due to, for example, competition with food production and environmental burdens of agriculture. Formate can be made from CO_2 and renewable electricity using electrochemical reduction. However, electrochemical production of formate has not yet been scaled-up and is not as energy-efficient as the electrochemical production of hydrogen (H_2) from water and electricity, which is already performed on a large scale (3).

H_2 is an attractive, byproduct-free sacrificial substrate for cofactor recycling. Molecular H_2 can be oxidized by organisms using hydrogenases. Some of the most extensively researched H_2-uptake hydrogenases are found in the hydrogen-oxidizing bacterium *Cupriavidus necator* H16 (formerly *Ralstonia eutropha*) (4). This bacterium possesses two types of oxygen-tolerant hydrogenases that provide the cells with reducing power: membrane-bound and soluble hydrogenases (5). The membrane-bound hydrogenase is located in the cytoplasmic membrane where it directly feeds electrons to the respiratory chain for ATP production by oxidative phosphorylation. The NAD-dependent hydrogenase resides in the cytoplasm and is therefore referred to as soluble hydrogenase (SH) (6, 7). The electrons and protons from H_2 can be directly transferred to NAD^+ by the SH, reducing NAD^+ to NADH while simultaneously oxidizing hydrogen (4).

C. necator H16 SH has been researched broadly for cofactor recycling using purified enzymes (8-12). Compared to purified enzymes, whole-cell biocatalysts can provide enzyme stabilization, as isolated intracellular enzymes typically lose activity more quickly than when they are in their natural cellular environments (13). Whole-cell systems can also have lower production costs by eliminating the need for enzyme purification or external addition of cofactors. Additionally, whole cells are generally more robust and exhibit better tolerance to inhibitors compared to purified enzymes. Whole cells were used in one of the earliest studies of SH-catalyzed cofactor recycling in the 1980s where

native *C. necator* cells reduced CO_2 to formate with a 30% yield (14). More recently, whole cells of recombinant *C. necator* have been employed as a biocatalyst by Oda et al. (15) and Assil-Companioni et al. (16) for reduction of hydroxyacetone to (*R*)-1,2-propanediol and for asymmetric C=C bond reduction of unsaturated cyclic ketones, respectively. However, given the limited extent of research and number of products, further studies are required to investigate *C. necator* as a whole-cell biocatalyst. In the current study, we show that the scope of hydrogen-driven reductive bioconversions can be broadened to encompass a new class of products, sugar alcohols, with xylitol as a particular example.

Xylitol ($C_5H_{12}O_5$) is a sugar alcohol used widely as a sweetener (17). It is currently produced chemically from D-xylose ($C_5H_{10}O_5$), which is the second most abundant sugar in lignocellulosic biomass (18). The chemical production of xylitol requires extensively purified D-xylose to avoid inactivation of the catalyst. In contrast, biotechnological production does not have this requirement and exhibits greater tolerance for inhibitors. Many yeasts, along with some bacteria and filamentous fungi, naturally reduce D-xylose to xylitol (18). However, numerous studies have focused on heterologous expression of D-xylose reductase (XR), aiming to increase yield and productivity of xylitol (19-23). All these studies use sugars to power the conversion, and to our knowledge H_2 has not been used as the electron and energy source for the D-xylose-to-xylitol conversion.

The objective of this study was to develop a whole-cell biocatalyst strain of *C. necator* for xylitol production using H_2 as the electron donor. To achieve this, XR from *Scheffersomyces stipitis* (formerly *Pichia stipitis*) was expressed in *C. necator* to allow the cells to convert D-xylose into xylitol (Figure 1). The native SH of *C. necator* enabled the H_2-driven cofactor recycling required for bioconversion. Resting (i.e., non-dividing) cells were used in the experiments. These viable cells exhibit reduced metabolic activity, which allows energy to be directed towards bioconversion instead of biomass accumulation (24). With the experimental set-up used, we achieved nearly full quantitative conversions.

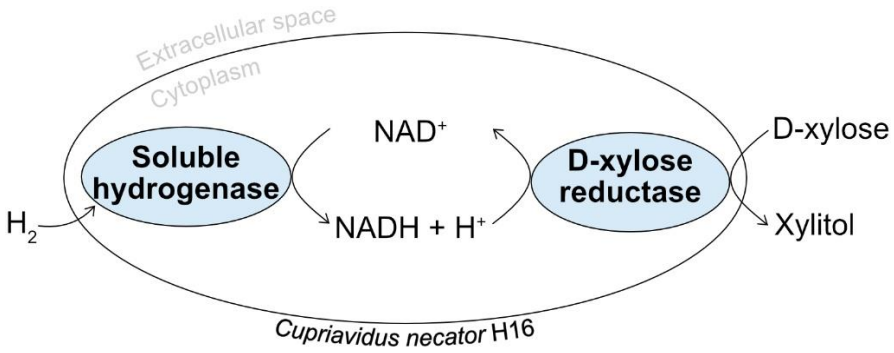

Figure 1. H_2-driven production of xylitol from D-xylose in whole cells of *Cupriavidus necator* H16 expressing D-xylose reductase from *Scheffersomyces stipitis.*

52 **Materials and methods**

53 **Strains and culture media**

54 Bacterial strains and plasmids used in this work are listed in Table 1 and the primers in Table S1 (see Additional file 1). *C.*
55 *necator* H16 strains were grown in either rich BD BBL™ Trypticase™ Soy Broth (TSB) or minimal AUT medium (25)
56 supplemented with 2 g/L fructose and glycerol (FG). Compared to the original AUT medium, the amount of $NiCl_2$ was
57 doubled and SL-6 trace elements were added (1:1000) (26). *Escherichia coli* DH10β was used for plasmid construction.
58 Tetracycline was added at a concentration of 10 µg/mL for *E. coli* and 5 µg/mL for *C. necator* when required. The sugars
59 and sugar alcohols used in the study were purchased from Sigma-Aldrich.

60 **Table 1.** Bacterial strains and plasmids used in the study. The strains with △*phaC* deletion are unable to produce
61 polyhydroxybutyrate (PHB) for carbon and energy storage.

Strain	**Relevant characteristics**	**Source or reference**
C. necator H16 △*phaCAB*	△*phaC1* △*phaA1* △*phaB1*	(27)
C. necator H16 △*phaC1*	△*phaC1*	(28)
C. necator H16 △*A0006*	△*phaC1* △*A0006*	This study
C. necator H16 △*phaCAB*_gfp	△*phaCAB* derivative, pPj5:GFP	This study
C. necator H16 △*phaC*_gfp	△*A0006* derivative, pPj5:GFP	This study
C. necator H16 △*phaCAB*_xr	△*phaCAB* derivative, pPj5:XRsti	This study
C. necator H16 △*phaC*_xr	△*A0006* derivative, pPj5:XRsti	This study
Plasmid		
pLO3	Suicide vector, sacB	(29)
pLO3-*A0006*	pLO3 derivative with 1100 bp upstream and downstream regions of *A0006*	This study
pPj5:GFP	pSEVA521 containing Pj5 promoter and GFP	(30)
pPj5:XRsti	pPj5:GFP derivative, GFP replaced with D-xylose reductase from *Scheffersomyces stipitis* (XRsti)	This study

62

63

64 **Strain construction**

65 XR from *Scheffersomyces* (*Pichia*) *stipitis* was ordered codon-optimized for *C. necator* from GenScript (Additional file 1:
66 Table S2) and PCR amplified with Q5 High-Fidelity 2X Master Mix (NEB). The backbone plasmid pSEVA521+Pj5:GFP and
67 the amplified insert were digested with *Spe*I-HF and *Hin*dIII-HF (NEB) and ligated using T4 DNA ligase (NEB) to gain
68 pPj5:XRsti. The verified plasmid was transformed into electrocompetent *C. necator* cells. For preparing competent cells,
69 *C. necator* was grown in 100 mL of TSB supplemented with 20 mM of fructose to an optical density at 600 nm (OD_{600}) of
70 0.6 and washed twice with 1 mM $MgSO_4$. The pellet was resuspended into 2 mL of 1 mM $MgSO_4$ and 1 mL of 60%
71 glycerol. Aliquots (50 µL) were stored in -80°C. Cells were mixed with plasmids (250 ng) in a 0.2 cm electroporation
72 cuvette (Bio-Rad), incubated 10 min on ice and electroporated with Electro Cell Manipulator ECM®630 (BTX) with the
73 following settings: 2.5 kV, 200 Ω and 25 µF. Super Optimal Broth with 20 mM fructose (950 µL) was added immediately
74 after electroporation and cells were incubated at 30°C and 180 rpm for 2-3 hours before plating on BBL™ Trypticase™
75 Soy Agar (TSA).

76 *C. necator* H16 △*A0006* was constructed from *C. necator* H16 △*phaC1* by deleting *A0006* with pLO3-based suicide vector
77 as previously described (29) (Additional file 1: Table S3). The △*A0006* restriction enzyme knockout increases
78 electroporation efficiency (31, 32) and is not expected to have any metabolic effects.

79 **XR activity assay**

80 For the XR activity assay, cells were grown overnight in TSB and then harvested by centrifugation (10 min, 2800 g). The
81 pellet was washed once with 50 mM potassium phosphate buffer (pH 7.5), resuspended into 1 mL of the same buffer
82 supplemented with cOmplete™ protease inhibitor (Roche) and moved into a 2 mL screw-cap tube with 400 µL of 0.5 mm
83 diameter glass beads. The cells were disrupted with FASTPREP-24 5G (MP Biomedicals) for 2x30sec at 6 m/s speed. After
84 disruption, the tube was centrifuged for 10 min at 16000 g, and the supernatant (soluble extract) was collected. Total
85 protein concentration was analyzed from the soluble extract by Quick Start™ Bradford Protein Assay (Bio-Rad) using
86 bovine serum albumin as the standard. XR activity assays were conducted in 96-well plates. The reaction mixture (330
87 µL) contained 0.15 mM of cofactor (NADH or NADPH), 50 mM potassium phosphate buffer (pH 6.0), 200 mM D-xylose
88 and an appropriate amount of soluble extract. Absorbance was measured at 340 mM using Epoch 2 Microplate
89 Spectrophotometer (BioTek). One unit of xylose reductase activity was defined as µmol of NAD(P)H oxidized per minute.

90 Specific activities were expressed as units per milligram of total protein. The results are given as averages of triplicate
91 assays.

92 **Bioconversions with resting cells**

93 Precultures were grown overnight in TSB media. FG media with tetracycline was inoculated to an initial OD_{600} of 0.1 and
94 grown for three days, reaching a final OD_{600} of approximately 4. The culture was centrifuged for 10 min at 2800 g and
95 washed twice with 100 mM sodium phosphate buffer (pH 7.0) to remove carbon and nitrogen sources. The cells were
96 resuspended in the same buffer with 30 g/L of substrate to an OD_{600} of 13-17, if not mentioned otherwise. This range of
97 OD_{600} corresponds approximately to a cell dry weight of 4.4-5.4 g/L. The prepared cell suspension (5 mL) was transferred
98 into an anaerobic serum bottle with a rubber stopper. D-xylose was the primary substrate, but one bioconversion was
99 also performed using L-arabinose and another using D-ribose. Three replicate bottles per bioconversion condition were
100 prepared.

101 For the first bioconversion experiments, 100 mL serum bottles were filled with H_2 using vacuum-gas cycles to reach
102 specific H_2 and oxygen (O_2) concentrations. As negative controls, bioconversions were performed under ambient air. The
103 bottles were incubated at 30°C and 150 rpm. Samples (200 µL) were taken by opening the rubber stopper and the bottles
104 were refilled with gasses after sampling. For bioconversion optimization, 50 mL serum bottles were filled with H_2 at the
105 start of the bioconversion by flushing with 100% H_2 at 0.5 mL min^{-1} for 2 minutes. Samples (200 µL) were taken using a
106 needle and syringe through the rubber stopper of sealed bottles. The approximate H_2 gas consumption was measured
107 after bioconversions by filling a 50 mL syringe with air and recording the volume of air aspirated into the bottle through
108 the syringe needle. Samples were centrifuged for 10 min at 16000 g and the supernatants were analyzed for sugars and
109 sugar alcohols.

110 **Calculation of H_2 consumption**

111 The amount of H_2 consumed was calculated from the approximated H_2 gas consumption (Equation 1):

112 $$n\ (\mathrm{H_2\ consumed}) = \frac{pV}{RT} \quad (1)$$

113 where *p* is the pressure (1 bar), *V* is the gas volume consumed (L), *R* is the gas constant (0.08314 L bar K^{-1} mol^{-1}) and *T* is
114 the temperature (298.15 K).

115

116 One mole of H_2 is needed to reduce one mole of xylose (Equation 2):

117 $$H_2 + C_5H_{10}O_5 = C_5H_{12}O_5 \quad (2)$$

118 The total amount of xylitol produced was calculated as the sum of the xylitol at the end of the bioconversion and the
119 xylitol in the fractions taken out during sampling. The ratio of xylitol production to H_2 consumption was calculated to
120 determine the proportion of energy and protons transferred from H_2 to xylitol.

121 **Analysis of sugars and sugar alcohols**

122 Two different high performance liquid chromatography (HPLC) systems were used for D-xylose and xylitol analysis:
123 Prominence-i LC-2030C (Shimadzu) equipped with Hi-Plex H 7.7x300 mm column (Agilent) at 45°C and 10 mM H_2SO_4 as
124 eluent at a flow rate of 1 ml min^{-1} and Vanquish Flex (Thermo Fisher Scientific) equipped with Aminex Fast Acid Analysis
125 and HPX-87H columns (Bio-Rad) at 55°C and 2 mM H_2SO_4 as the eluent at a flow rate of 0.5 ml min^{-1}. An injection volume
126 of 10 µL was used in both HPLCs and the compounds were detected with a refractive index detector. L-arabinose, L-
127 arabitol, D-ribose and ribitol were analyzed with high pressure ion chromatography (HPIC) Dionex ICS-6000 (Thermo
128 Fisher Scientific) with CarboPac PA20 column (Thermo Fisher Scientific) at 30°C and 10 mM KOH as the eluent at a flow
129 rate of 0.5 ml min^{-1}. An injection volume of 2.5 µL was used and the compounds were detected with an electrochemical
130 detector. Conversion yields were calculated by dividing the final molar concentration of xylitol by the initial molar
131 concentration of xylose.

132 **Results**

133 **Xylose reductase from *S. stipitis* is functionally produced in *C. necator* H16**

134 In this study, two *C. necator* strains, △*phaC* and △*phaCAB*, with partial or full knockouts of the native pathway for storage
135 polymer polyhydroxybutyrate (PHB) formation, were used to avoid the accumulation of this by-product. Before
136 constructing the XR expressing strains, it was confirmed that the host strains cannot grow on C5 sugars and sugar
137 alcohols used in the study (Additional file 1: Fig. S1). Both strains were then transformed with the plasmids pPj5:XR,
138 carrying the codon-optimized XR from *S. stipitis,* and pPj5:GFP, as a negative control. Strains were cultivated
139 heterotrophically, and their soluble extracts were tested for XR activity. The soluble extracts of both XR strains showed
140 reductase activity with both NADPH and NADH cofactors, whereas no activity was detected in the negative control strains
141 (Table 2). Codon-optimized XR from *Candida parapsilosis* was also expressed in the host strains, but no activity was
142 detected (data not shown).

143 **Table 2.** Specific D-xylose reductase activities of soluble extracts with NADPH or NADH as cofactors (U/mg). The average

144 from three measurements is shown with the standard deviation. No activity could be detected in the negative controls.

Strain	NADPH	NADH
△*phaCAB*_xr	0.71±0.20	0.48±0.01
△*phaC*_xr	0.49±0.01	0.41±0.03

145

146 **Xylose is fully converted to xylitol by *C. necator* △*phaCAB***

147 The first bioconversion experiment was performed at 30 g/L D-xylose by both *C. necator* strains: △*phaCAB*_xr and

148 △*phaC*_xr. The suspensions were incubated under H_2 (85% H_2 + 15% air) or 100% ambient air. Under H_2, the

149 △*phaCAB*_xr strain reached almost complete bioconversion to xylitol within 16 days, whereas the △*phaC*_xr strain

150 converted 74% of the provided D-xylose at the same time (Figure 2). Therefore, further bioconversions were performed

151 using the △*phaCAB*_xr strain. D-xylose was also converted to xylitol in the absence of H_2 by both strains, but the

152 conversion yields were under 21% after 16 days. This demonstrated successful cofactor recycling in resting cells of *C.*

153 *necator* using H_2.

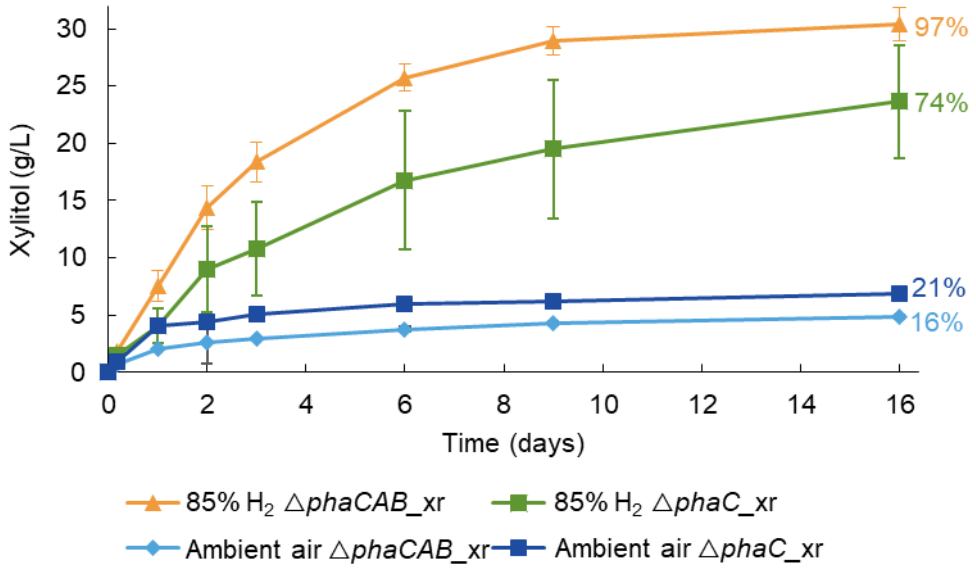

154

155 **Figure 2.** H_2-driven production of xylitol by *C. necator* △*phaCAB*_xr and △*phaC*_xr. The initial concentration of D-xylose

156 was ~30 g/L in 100 mM sodium phosphate buffer (pH 7.0) with the cells at OD_{600} of 17 (△*phaCAB*_xr) and 15 (△*phaC*_xr).

157 The used gas mixture consisted of 85% H_2, 12% N_2, and 3% O_2 while ambient air contains 78% N_2 and 21% O_2. The average

158 from three bioconversions is shown with the standard deviation. The percentages represent the final conversion yields,
159 calculated by dividing the xylitol concentration measured at the final time point by the xylose concentration at the start
160 of the experiment.

161 **Oxygen is not required for the bioconversion**

162 Since oxygen, acting as an electron acceptor, can provide the cells with energy via oxidative phosphorylation, we
163 examined the effect of oxygen concentration on the conversion rate. Three different oxygen concentrations (0, 1, and
164 4%) were tested. The conversion rates and yields showed little variation between the different oxygen concentrations
165 (Figure 3), with over 85% conversion yields being reached within 10 days in all conditions. After confirming that oxygen
166 was not required for the bioconversion, it was tested whether the amount of H_2 was a limiting factor. Bioconversions
167 with multiple H_2 flushes during the experiment were compared to bioconversions with a single H_2 flush at the start. The
168 results showed that multiple H_2 flushes failed to improve the conversion yield (Additional file 1: Fig. S2). Therefore,
169 further bioconversions were conducted with only an initial H_2 flush.

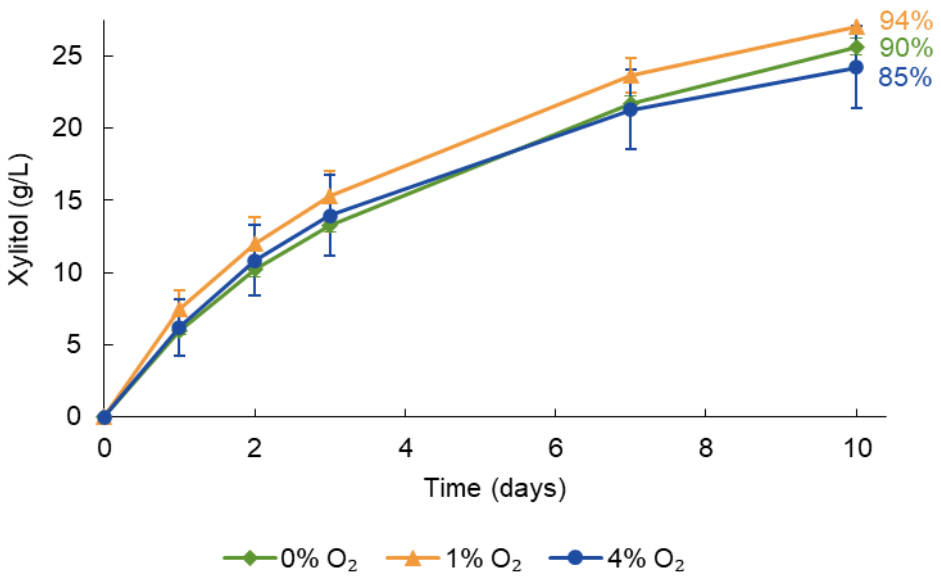

170

171 **Figure 3.** H_2-driven production of xylitol by *C. necator* △*phaCAB* on different oxygen concentrations. The reaction
172 mixtures contained initially ~30 g/L of D-xylose in 100 mM sodium phosphate buffer (pH 7.0) with cells at OD_{600} of 16.
173 The used gas mixtures consisted of 0% O_2 and 100% H_2, 1% O_2, 2% N_2, and 97% H_2 or 4% O_2, 13% N_2, and 83% H_2. The
174 average from three bioconversions is shown with the standard deviation. The percentages represent the final conversion
175 yields, calculated by dividing the xylitol concentration measured at the final time point by the xylose concentration at
176 the start of the experiment.

177 **Higher initial sugar concentration can speed up the bioconversion rate**

178 Four different D-xylose concentrations were tested to evaluate their impact on xylitol production rates. With increasing
179 xylose concentration, the rate of conversion increased (Figure 4). The highest xylitol productivity in the first 48 hours
180 (0.7 g L^{-1} h^{-1}) was reached with the highest xylose concentration used (114 g/L D-xylose). However, conversion proceeded
181 faster at a lower xylose concentration: 99% of 13 g/L of D-xylose was converted to xylitol in 7 days while 83% of 34 g/L
182 D-xylose was converted within the same time.

183 In samples with the highest xylose concentrations (66 and 114 g/L), the final xylitol concentration reached 46 g/L. We
184 hypothesized that H_2 in the headspace was limiting and that measuring H_2 consumption could allow us to estimate the
185 electron conversion efficiency of hydrogen into xylitol. On average, 30 mL of gas was consumed under both conditions,
186 equivalent to 1.2 mmol of H_2. Given that 0.2 mmol of xylitol was produced without H_2 (as shown in Figure 2) and 1.3
187 mmol was produced in total, it can be assumed that 1.1 mmol of xylitol was produced with the help of H_2 under both
188 conditions. Consequently, more than 90% of the energy derived from H_2 was spent for the bioconversion, as one mole
189 of H_2 is required to reduce one mole of xylose (Additional File 1: Full calculations). We wish to highlight that this
190 calculation is an approximation.

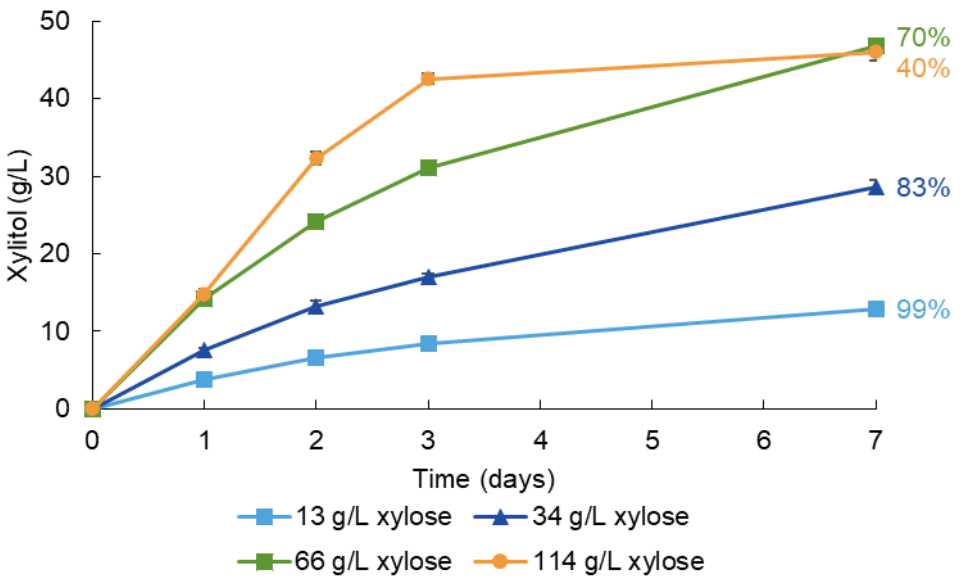

191

192 **Figure 4.** H_2-driven production of xylitol by *C. necator* △*phaCAB* at different D-xylose concentrations. The reaction
193 mixtures were composed of 13, 34, 66, and 114 g/L of D-xylose in 100 mM sodium phosphate buffer (pH 7.0) and cells
194 at OD_{600} of 13-15. The headspace contained 100% H_2. The average from three bioconversions is shown with the standard

195 deviation. The percentages represent the final conversion yields, calculated by dividing the xylitol concentration
196 measured at the final time point by the xylose concentration at the start of the experiment.

197 **Increased cell concentration enhances the rate of bioconversion**

198 So far, all bioconversions in this study were conducted with a cell concentration range of OD_{600} 13-17. The effect of the
199 amount of the whole-cell biocatalyst was examined at lower and higher cell concentrations: OD_{600} 7 and 60. With the
200 highest cell concentration, 91% conversion of 30 g/L D-xylose to xylitol was achieved in 7 days (Figure 5). Increasing the
201 cell concentration had a positive effect also on the xylitol production rate. In the first 24 hours, the production rates
202 were 0.5 g L^{-1} h^{-1} and 0.1 g L^{-1} h^{-1} for the highest and lowest cell concentrations used, respectively.

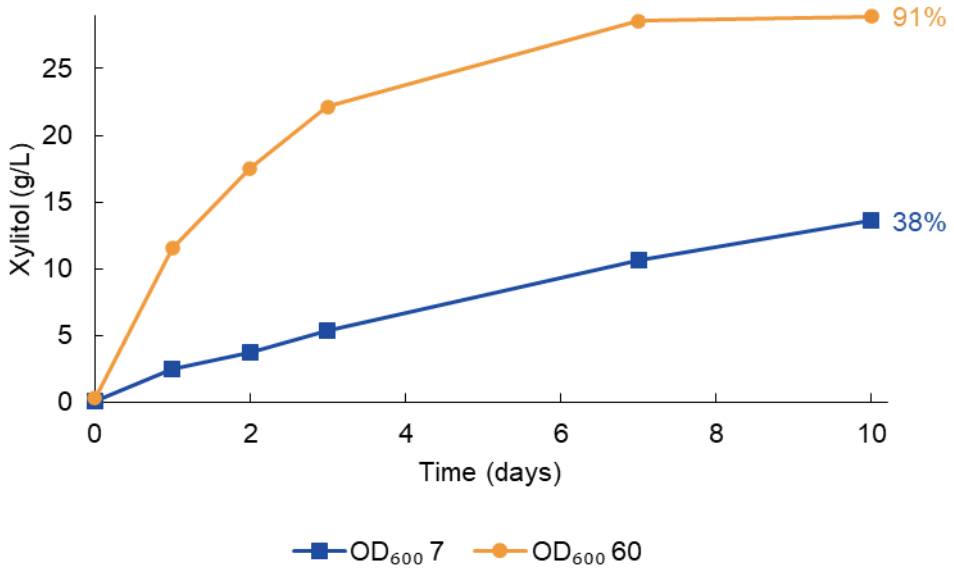

203

204 **Figure 5.** H_2-driven production of xylitol by *C. necator* △*phaCAB* at different cell concentrations. The initial concentration
205 of D-xylose was ~30 g/L. The conversions were carried out in a 100 mM sodium phosphate buffer (pH 7.0) under 100%
206 H_2. The average from three bioconversions is shown with the standard deviation. The percentages represent the final
207 conversion yields, calculated by dividing the xylitol concentration measured at the final time point by the xylose
208 concentration at the start of the experiment.

209 **Arabinose and ribose are reduced to sugar alcohols by the resting cells**

210 *S. stipitis* XR is also known to convert L-arabinose and D-ribose into their respective sugar alcohols (33). Therefore, we
211 examined whether *C. necator* harboring the xylose reductase could also be used as a biocatalyst for these conversions.

212 Both sugars were successfully reduced to their corresponding sugar alcohols, with the production rates of L-arabitol and
213 ribitol being only slightly lower than those for xylitol (Figure 6).

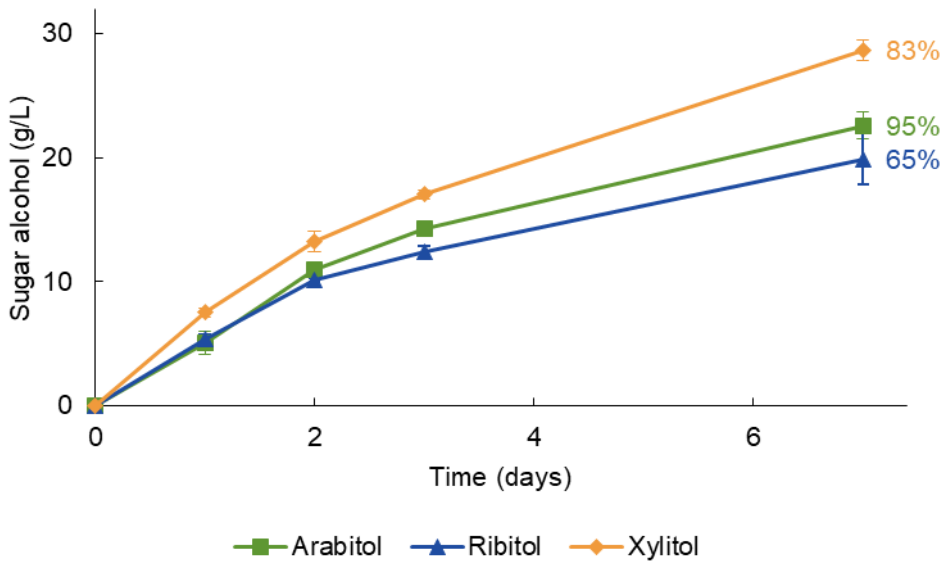

214

215 **Figure 6.** H_2-driven production of L-arabitol, ribitol and xylitol by C. necator △*phaCAB*. The initial concentrations of L-
216 arabinose, D-ribose and D-xylose were 24, 30 and 34 g/L, respectively, and the corresponding cell densities (OD_{600}) were
217 15, 15, and 13. The experiments were carried out in a 100 mM sodium phosphate buffer (pH 7.0) under 100% H_2. The
218 average from three bioconversions is shown with the standard deviation. The percentages represent the final conversion
219 yields, calculated by dividing the xylitol concentration measured at the final time point by the xylose concentration at
220 the start of the experiment.

221 **Discussion**

222 This study aimed to advance the development of *C. necator* as a H_2-driven whole-cell biocatalyst. We demonstrated
223 nearly complete reduction of 30 g/L of D-xylose to xylitol with 97% conversion yield in resting cells using H_2 for cofactor
224 regeneration (Figure 2). The effects of different parameters on xylitol production were studied to improve the production
225 rates. Additionally, it was shown that the system can convert L-arabinose and D-ribose into their respective sugar
226 alcohols (Figure 6).

227 *C. necator* accumulates polyhydroxybutyrate (PHB) as a carbon and energy storage compound. To avoid this
228 accumulation, which could also lead to cofactor oxidation, PHB-negative strains △*phaCAB* and △*phaC* of *C. necator* were
229 used as hosts. Comparison of the △*phaCAB*_xr *and* △*phaC*_xr strains revealed that deletion of the whole PHB pathway

230 (*phaCAB*) enhanced both the bioconversion rate and yield (Figure 2). In the △*phaC* knock-out strain, it is possible that
231 some of the reducing equivalents from H_2 were consumed by the NAD(P)H-utilizing acetoacetyl-CoA reductase (PhaB)
232 of the PHB pathway. The advantage of knocking out more than just the *phaC* gene has also been observed in earlier
233 studies in non-resting cells of *C. necator*. For instance, complete deletion of the PHB pathway was found to be beneficial
234 for resveratrol production in *C. necator,* whereas deletion of only the *phaC* gene did not improve the titer compared to
235 the wild type (34).

236 Oxygen is essential for ATP production from H_2 in *C. necator*. Although the bioconversion reaction itself does not require
237 ATP, it was hypothesized that the cells would require some ATP for cell maintenance. However, the results suggest
238 otherwise (Figure 3). This outcome is advantageous for industrial applications, as oxygen-free production mitigates the
239 risk associated with flammability of H_2-O_2 mixtures. The experiments also demonstrated efficient transfer of nearly all
240 hydrogen-derived electrons into the product. When enough H_2 was present in the headspace, nearly full bioconversion
241 of xylose could be demonstrated. However, liquid solubility of H_2 is low and hence may still limit the rate of conversion.
242 To test this, bioconversions could be performed under elevated pressure, where H_2 solubility is increased, but
243 unfortunately it was not possible to test this with the current experimental set-up. Additionally, mass transfer of H_2 to
244 the liquid phase can be significantly improved by using optimized bioreactors equipped with specialized gas spargers
245 and impellers (35).

246 The most significant improvements in the bioconversion rate were achieved by increasing the cell concentration and
247 xylose concentration. This is not surprising, as a higher cell concentration provides more catalyst for the conversion to
248 occur, and an increased substrate concentration boosts the reaction rate until enzyme saturation is reached. The most
249 efficient xylitol production systems reported in the literature have reached higher xylitol productivity than the 0.7 g L^{-1}
250 h^{-1} observed in this study. Whole-cell systems have reached up to 12 g L^{-1} h^{-1} (36), while *in vitro* systems have achieved
251 21 g L^{-1} h^{-1} (23). At a similar cell density to that used in this study, recombinant *E. coli* cells, coexpressing a D-xylose
252 reductase and a glucose dehydrogenase, produced xylitol at 6.4 g L^{-1} h^{-1}. In this optimized process, a 100% yield was
253 achieved at an initial D-xylose concentration of 200 g/L using glucose for cofactor recycling (23). Factors that could
254 account for this include lower enzyme activities, slower substrate and product transport into and outside of the cell, and
255 particularly the aforementioned poor H_2 solubility. Observing the SDS-PAGE gel of Jin et al., it seems that their XR level
256 in the cell was much higher than in this study (Additional file 1: Fig. S3). Although one of the strongest promoters
257 currently known for *C. necator* was used in the present study (30, 37), stronger expression of XR could improve the

258 bioconversion rates. The expression systems for *C. necator* need further development to achieve the expression levels
259 obtained with *E. coli*. On the other hand, the xylose and xylitol transport systems of *E. coli* are likely more efficient than
260 those of *C. necator* because *E. coli* can natively grow on xylose whereas *C. necator* cannot. A BLAST search of the *C.*
261 *necator* H16 genome using the D-xylose specific transport systems of *E. coli* (XylE and XylFGH) yielded no matches,
262 suggesting that *C. necator* lacks xylose-specific transporters. Xylose is likely transported into the cells by a sugar
263 transporter with side activity for xylose. Hence, heterologous introduction of a xylose transporter could be considered
264 for future studies to further improve bioconversion rates.

265 The specific activity of XR with NADPH was higher compared to NADH (Table 2). The same result has been observed
266 previously by Verduyn et al. (33). Using NADPH-producing SH, instead of the native NADH-producing SH, with NADPH-
267 dependent oxidoreductases could increase the rate of the bioconversion. The NAD^+-specific SH from *C. necator* has been
268 engineered to also accept $NADP^+$, but its $NADP^+$-reducing activity would need to be increased (12). Another option is to
269 use NADH-preferring oxidoreductases or to engineer them to have this preference, ensuring high activity towards NADH.

270 This article presented the first whole-cell, H_2-driven biocatalysis study using a PHB-negative *C. necator* strain as the host.
271 Direct comparison of this work to the few prior studies is challenging due to differences in experimental setups, product
272 types, enzyme kinetics, and strains used. Oda et al. (15) reported a productivity of 0.9 g L^{-1} h^{-1} for (*R*)-1,2-propanediol,
273 which is within the same order of magnitude as our findings. Whole-cell cofactor recycling using SH has not only been
274 done in *C. necator*. Lonsdale et al. (38) expressed SH from *C. necator* in *Pseudomonas putida* to perform H_2-driven
275 bioconversion of n-octane to 1-octanol. The cofactor recycling proved to be effective, resulting in a threefold increase
276 in 1-octanol production in the presence of H_2. However, the yield and rate of bioconversions they achieved were
277 significantly lower than the ones in this study; Lonsdale et al. reported a maximum productivity of 0.01 g L^{-1} h^{-1}, about
278 100-fold lower than the rates we and Oda et al. achieved.

279 The limited amount of research in this area offers a wide range of opportunities for improving these organisms to
280 perform H_2-driven bioconversions towards industrial applications. Bioconversion rates can likely be significantly
281 improved using hosts with improved enzyme activities, elevated pressures, higher cell concentrations and optimized
282 bioreactor designs that enhance hydrogen solubility.

283

284

Conclusions

Cofactor recycling via hydrogenases represents a promising alternative for traditional bioconversion systems because of its atom efficiency, lack of by-products and the prospects of H_2 becoming a renewable platform chemical of the future. This study demonstrated H_2-driven bioconversion of D-xylose to xylitol in XR expressing *C. necator* strain. 30 g/L of D-xylose was almost fully converted into xylitol by this system. It was shown that nearly all the energy from H_2 is harnessed by the bioconversion, demonstrating the potential of the *C. necator* system as an efficient H_2-driven biocatalyst for sugar alcohol production and potentially other products.

Data availability

The datasets generated and analyzed during the current study are available from the corresponding author on reasonable request.

Competing interests

The authors declare that they have no competing interests.

Funding

This work was supported by the Research Council of Finland (KNALLRED—Hydrogen powered reductive biosyntheses and biotransformations by an engineered Knallgas bacterium, grant number 342124).

Authors' contributions

All authors designed research. TJ conducted experiments, data analysis, and wrote the manuscript. All authors revised and approved the manuscript.

Acknowledgements

The authors thank Enrico Orsi for the *C. necator* △*phaCAB* strain, Guillermo Bordanaba Florit for constructing the *C. necator* H16 △*A0006* strain, Victor de Lorenzo's lab for the SEVA plasmid, and Ton van Gelder for the help with HPLC analyses. We also thank Solar Foods, especially Juha-Pekka Pitkänen, for the fruitful discussions and the bioeconomy research infrastructures of Aalto University for the support.

Additional file 1: Table S1. Oligonucleotide primers used in the study. **Table S2.** Synthesized xylose reductase gene used in this study originating from *Scheffersomyces stipitis*. **Table S3.** Upstream and downstream regions of *A0006* used to

create *C. necator* H16 △*A0006*. **Figure S1.** The growth of *C. necator* strains △*phaCAB* and △*phaC* on different sugars and sugar alcohols (100 mM). **Figure S2.** Comparison of bioconversion with a single H_2 flush at the start and H_2 flush after every sampling. **Figure S3.** SDS-PAGE analysis of soluble extracts by *C. necator* H16 strains. **Full calculations.**

References

1. Wang X, Saba T, Yiu HHP, Howe RF, Anderson JA, Shi J. Cofactor NAD(P)H regeneration inspired by heterogeneous pathways. Chem. 2017; doi:10.1016/j.chempr.2017.04.009
2. van der Donk WA, Zhao H. Recent developments in pyridine nucleotide regeneration. Curr Opin Biotechnol. 2003; doi:10.1016/s0958-1669(03)00094-6
3. Stöckl M, Claassens NJ, Lindner SN, Klemm E, Holtmann D. Coupling electrochemical CO_2 reduction to microbial product generation - identification of the gaps and opportunities. Curr Opin Biotechnol. 2022; doi:10.1016/j.copbio.2021.11.007
4. Lubitz W, Ogata H, Rudiger O, Reijerse E. Hydrogenases. Chem Rev. 2014; doi:10.1021/cr4005814
5. Lenz O, Lauterbach L, Frielingsdorf S, Friedrich B. Oxygen-tolerant hydrogenases and their biotechnological potential. In: Rögner M, editor. Biohydrogen. Berlin: Walter de Gruyter GmbH; 2015.
6. Jugder BE, Chen Z, Ping DT, Lebhar H, Welch J, Marquis CP. An analysis of the changes in soluble hydrogenase and global gene expression in *Cupriavidus necator* (*Ralstonia eutropha*) H16 grown in heterotrophic diauxic batch culture. Microb Cell Fact. 2015; doi:10.1186/s12934-015-0226-4
7. Cramm R. Genomic view of energy metabolism in *Ralstonia eutropha* H16. J Mol Microbiol Biotechnol. 2009; doi:10.1159/000142893
8. Holzer AK, Hiebler K, Mutti FG, Simon RC, Lauterbach L, Lenz O, et al. Asymmetric biocatalytic amination of ketones at the expense of NH_3 and molecular hydrogen. Org Lett. 2015; doi:10.1021/acs.orglett.5b01154
9. Ratzka J, Lauterbach L, Lenz O, Ansorge-Schumacher MB. Systematic evaluation of the dihydrogen-oxidising and NAD^+-reducing soluble [NiFe]-hydrogenase from *Ralstonia eutropha* H16 as a cofactor regeneration catalyst. Biocatal Biotransform. 2011; doi:10.3109/10242422.2011.615393
10. Al-Shameri A, Willot SJ, Paul CE, Hollmann F, Lauterbach L. H_2 as a fuel for flavin- and H_2O_2-dependent biocatalytic reactions. Chem Commun. 2020; doi:10.1039/d0cc03229h
11. Cha J, Bak H, Kwon I. Hydrogen-fueled CO_2 reduction using oxygen-tolerant oxidoreductases. Front Bioeng Biotechnol. 2022; doi:10.3389/fbioe.2022.1078164
12. Preissler J, Reeve HA, Zhu T, Nicholson J, Urata K, Lauterbach L, et al. Dihydrogen-driven NADPH recycling in imine reduction and P450-catalyzed oxidations mediated by an engineered O_2-tolerant hydrogenase. ChemCatChem. 2020; doi:10.1002/cctc.202000763
13. Lin B, Tao Y. Whole-cell biocatalysts by design. Microb Cell Fact. 2017; doi:10.1186/s12934-017-0724-7
14. Klibanov AM, Alberti BN, Zale SE. Enzymatic synthesis of formic acid from H_2 and CO_2 and production of hydrogen from formic acid. Biotechnol Bioeng. 1982; doi:10.1002/bit.260240104
15. Oda T, Oda K, Yamamoto H, Matsuyama A, Ishii M, Igarashi Y, et al. Hydrogen-driven asymmetric reduction of hydroxyacetone to (R)-1,2-propanediol by *Ralstonia eutropha* transformant expressing alcohol dehydrogenase from *Kluyveromyces lactis*. Microb Cell Fact. 2013; doi:10.1186/1475-2859-12-2
16. Assil-Companioni L, Schmidt S, Heidinger P, Schwab H, Kourist R. Hydrogen-driven cofactor regeneration for stereoselective whole-cell C=C bond reduction in *Cupriavidus necator*. ChemSusChem. 2019; doi:10.1002/cssc.201900327
17. da Silva S, Chandel A. D-Xylitol: fermentative production, application and commercialization. 1st ed. Heidelberg: Springer-Verlag; 2012.

18. Narisetty V, Cox R, Bommareddy R, Agrawal D, Ahmad E, Pant KK, et al. Valorisation of xylose to renewable fuels and chemicals, an essential step in augmenting the commercial viability of lignocellulosic biorefineries. Sustain Energ Fuels. 2022; doi:10.1039/d1se00927c

19. Hallborn J, Walfridsson M, Airaksinen U, Ojamo H, Hahn-Hägerdal B, Penttilä M, et al. Xylitol production by recombinant *Saccharomyces cerevisiae*. Nat Biotechnol. 1991; doi:10.1038/nbt1191-1090

20. Nyyssölä A, Pihlajaniemi A, Palva A, von Weymarn N, Leisola M. Production of xylitol from D-xylose by recombinant *Lactococcus lactis*. J Biotechnol. 2005; doi:10.1016/j.jbiotec.2005.03.014

21. Cirino PC, Chin JW, Ingram LO. Engineering *Escherichia coli* for xylitol production from glucose-xylose mixtures. Biotechnol Bioeng. 2006; doi:10.1002/bit.21082

22. Sasaki M, Jojima T, Inui M, Yukawa H. Xylitol production by recombinant *Corynebacterium glutamicum* under oxygen deprivation. Appl Biochem Biotechnol. 2010; doi:10.1007/s00253-009-2372-2

23. Jin LQ, Xu W, Yang B, Liu ZQ, Zheng YG. Efficient biosynthesis of xylitol from xylose by coexpression of xylose reductase and glucose dehydrogenase in *Escherichia coli*. Appl Biochem Biotechnol. 2019; doi:10.1007/s12010-018-2878-0

24. Julsing MK, Kuhn D, Schmid A, Buhler B. Resting cells of recombinant *E. coli* show high epoxidation yields on energy source and high sensitivity to product inhibition. Biotechnol Bioeng. 2012; doi:10.1002/bit.24404

25. Lenz O, Lauterbach L, Frielingsdorf S. O_2-tolerant [NiFe]-hydrogenases of *Ralstonia eutropha* H16: physiology, molecular biology, purification, and biochemical analysis. Methods Enzymol. 2018; doi:10.1016/bs.mie.2018.10.008

26. Atlas RM. Handbook of microbiological media. 4th ed. Washington DC: Taylor & Francis; 2010.

27. Collas F, Dronsella BB, Kubis A, Schann K, Binder S, Arto N, et al. Engineering the biological conversion of formate into crotonate in *Cupriavidus necator*. Metab Eng. 2023; doi:10.1016/j.ymben.2023.06.015

28. Lütte S, Pohlmann A, Zaychikov E, Schwartz E, Becher JR, Heumann H, et al. Autotrophic production of stable-isotope-labeled arginine in Ralstonia eutropha strain H16. Appl Environ Microbiol. 2012; doi:10.1128/AEM.01972-12

29. Lenz O, Friedrich B. A novel multicomponent regulatory system mediates H_2 sensing in *Alcaligenes eutrophus*. Proc Natl Acad Sci. 1998; doi:10.1073/pnas.95.21.12474

30. Claassens NJ, Bordanaba-Florit G, Cotton CAR, De Maria A, Finger-Bou M, Friedeheim L, et al. Replacing the Calvin cycle with the reductive glycine pathway in *Cupriavidus necator*. Metab Eng. 2020; doi:10.1016/j.ymben.2020.08.004

31. Xiong B, Li Z, Liu L, Zhao D, Zhang X, Bi C. Genome editing of *Ralstonia eutropha* using an electroporation-based CRISPR-Cas9 technique. Biotechnol Biofuels. 2018; doi:10.1186/s13068-018-1170-4

32. Vajente M, Clerici R, Ballerstedt H, Blank LM, Schmidt S. Using *Cupriavidus necator* H16 to provide a roadmap for increasing electroporation efficiency in non-model bacteria. bioRxiv. 2024; doi:10.1101/2024.05.27.596136

33. Verduyn C, Van Kleef R, Frank J, Schreuder H, Van Dijken JP, Scheffers WA. Properties of the NAD(P)H-dependent xylose reductase from the xylose-fermenting yeast *Pichia stipitis*. Biochem J. 1985; doi:10.1042/bj2260669

34. Jang Y, Lee YJ, Gong G, Lee SM, Um Y, Kim KH, et al. Carbon dioxide valorization into resveratrol via lithoautotrophic fermentation using engineered *Cupriavidus necator* H16. Microb Cell Fact. 2024; doi:10.1186/s12934-024-02398-x

35. Tanaka K, Ishizaki A, Kanamaru T, Kawano T. Production of poly(D-3-hydroxybutyrate) from CO_2, H_2, and O_2 by high cell density autotrophic cultivation of *Alcaligenes eutrophus*. Biotechnol Bioeng. 1995; doi:10.1002/bit.260450312

36. Kwon SG, Park SW, Oh DK. Increase of xylitol productivity by cell-recycle fermentation of *Candida tropicalis* using submerged membrane bioreactor. J Biosci Bioeng. 2006; doi:10.1263/jbb.101.13

37. Gruber S, Hagen J, Schwab H, Koefinger P. Versatile and stable vectors for efficient gene expression in *Ralstonia eutropha* H16. J Biotechnol. 2014; doi:10.1016/j.jbiotec.2014.06.030

406 38. Lonsdale TH, Lauterbach L, Honda Malca S, Nestl BM, Hauer B, Lenz O. H_2-driven
407 biotransformation of n-octane to 1-octanol by a recombinant *Pseudomonas putida* strain co-synthesizing an
408 O_2-tolerant hydrogenase and a P450 monooxygenase. Chem Commun. 2015; doi:10.1039/c5cc06078h

409

Additional file 1

H_2-driven xylitol production in *Cupriavidus necator* H16

Tytti Jämsä[1,*], Nico J. Claassens[2], Laura Salusjärvi[1], Antti Nyyssölä[1]

[1] VTT Technical Research Centre of Finland Ltd., Tekniikantie 21, 02150 Espoo, Finland

[2] Laboratory of Microbiology, Wageningen University, Stippeneng 4, 6708WE Wageningen, the Netherlands

*Correspondence to Tytti Jämsä: tytti.jamsa@vtt.fi

Table S1. Oligonucleotide primers used in the study.

Primer	5' to 3' sequence	Details
oXR1	CCCAAGCTTTTAAAAGGGGAGGTATTTCTATGCCGTCGATCAAGCTGAA	PCR of synthesized *S. stipitis* XR for cloning
oXR2	CTAGACTAGTACCCCTTCCTTACACGAAGA	PCR of synthesized *S. stipitis* XR for cloning
oSEVA_F	TCTAGGGCGGCGGAT	Colony PCR
oSEVA_R	CTGGATTCTCACCAATAAAAAACG	Colony PCR

Table S2. Synthesized xylose reductase gene used in this study originating from *Scheffersomyces stipitis*. Codon-optimized for *C. necator* (957 bp). The original sequence is associated with GeneID 4839234.

Name	Nucleotide sequence
XRsti	ATGCCGTCGATCAAGCTGAACTCGGGCTACGACATGCCGGCCGTGGGCTTCGGCTGCTGG AAGGTGGACGTGGACACCTGCTCGGAACAGATCTACCGCGCCATCAAGACCGGCTACCGC CTGTTCGACGGCGCCGAGGACTACGCCAACGAAAAGCTGGTGGGCGCCGGCGTGAAGAAG GCCATCGACGAGGGCATCGTGAAGCGCGAAGACCTGTTCCTGACCTCGAAGCTGTGGAAC AACTACCACCACCCGGACAACGTGGAGAAGGCCCTGAACCGCACCCTGAGCGACCTGCAG GTGGACTACGTGGACCTGTTCCTGATCCACTTCCCGGTGACCTTCAAGTTCGTGCCGCTG GAGGAAAAGTACCCGCCGGGCTTCTACTGCGGCAAGGGCGACAACTTCGACTACGAGGAC GTGCCGATCCTGGAAACCTGGAAGGCCCTGGAGAAGCTGGTGAAGGCCGGCAAGATCCGC TCGATCGGCGTGTCGAACTTCCCCGGCGCCCTGCTGCTGGACCTGCTGCGCGGCGCAACC ATCAAGCCGTCGGTGCTGCAGGTGGAACACCACCCGTACCTGCAGCAGCCGCGCCTGATC GAGTTCGCCCAGAGCCGCGGCATCGCCGTGACCGCCTACTCGAGCTTCGGCCCGCAGTCG TTCGTGGAGCTGAACCAGGGCCGCGCCCTGAACACCAGCCCGCTGTTCGAGAACGAAACC ATCAAGGCCATCGCCGCCAAGCACGGCAAGAGCCCGGCCCAGGTGCTGCTGCGCTGGTCG AGCCAGCGCGGCATCGCCATCATCCCGAAGTCGAACACCGTGCCGCGCCTGCTGGAAAAC AAGGACGTGAACAGCTTCGACCTGGACGAGCAGGACTTCGCCGACATCGCCAAGCTGGAC ATCAACCTGCGCTTCAACGACCCGTGGGACTGGGACAAGATCCCGATCTTCGTGTAA

Table S3. Upstream and downstream regions of *A0006* used to create *C. necator* H16 △*A0006.*

Description	5’ to 3’ sequence
Upstream of *A0006*	CAAAGCTGGGCCGGATGCTGTGCGTGCTGCTGAAGGCGAAACGATACTGCTGTGGGACGG TTCGAACGCTGGGGAATTCTTCAGGTCCAAGGTCGGGTTGGTTGCTTCGACGATGACGAA GATTTCTCCGAGCAGTGTTTTTCGTCCGGCATACTTTTTTCATGTCGCCAAGCAAGCTGA GCGATTCCTGAAGGCTCAAACCAATGGCACTGGCATTCCACACGTTGACCGAGAGCTTCT CGAGGGGATAAAGGTCTTTTGTCCTGGCTCTACGGAGCAGCAATTACTTGCGGAAATCCT CGACACTCTCGACACCGCCATCTACGAAACTGAAGCGATCATCGCCAAGCTCAAGGCGGT CAAGCAAGGCCTGCTGCATGACCTCTTGACGCGCGGCATCGACGCCAACGGCGAATTGCG CCCACCTCAGGCCGAGGCACCGCATCTCTACGAGTCGTCACCGTTGGGTTGGATTCCGAA TGAGTGGGGTCTTGCTCCTACAGCAACTCGCTGCCATCTGATAACCAAAGGCACTACCCC TGCGGCTAATGAGATGTGGCAGGGTGGCGCGGGAATTAGGTTTCTGCGAGTCGATAATCT TTCTTTCGATGGACAACTGGATCTAGATGCAAGCACGTTTCGAGTTAGCCTTGCCACGCA CAAAGGTTTTCTGGCTCGTTCAAGATGCCTTGAAGGTGATGTGCTGACGAACATCGTTGG CCCACCTCTAGGGAAACTGGGGCTTGTTACCAAAGAAATTGGTGAGGTCAATATTAATCA AGCAATTGCGTTATTTCGACCAACCGAACAACTACTGCCAAAGTTCCTATTAATCTGGCT TAGTAGCTCAATCTCGCAGTCTTGGCTGAGGAACCGAGCCAAGCAGACGTCGGGACAAGT GAATCTGACCCTCGCTCTATGCCAGGAGCTTCCTCTACCTCGGATGACGATCAATGAGCA ACAGGCAATCGTTGACCGAGTTGATGCCGCGCAGGAACAAATCTGGTGTGAGGAGGAACT GATCCGAAAGATGCGACTTGAGAAATCTGGCCTTATGGATGACCTCCTCACCGGCCGCGT CCGCGTCAAGCCGCAGCTGGCGGAAACCAAACAAGCAGGGAGCGCCTGATG
Downstream of *A0006*	GCGCCTGATGCACGACAAGCTGATGCAGGTGTGATTCGATGCCTTCGCCGGTGAAATTGC CAAGCCTTCAGATCGGTGACCTCCGGTTCACGCTCCAGCGGAGCGCGCGCCGCAGAACTA TGCAGATCACCGTGGAGCGCAGTGGCGACTTGATGCTCTGCGCACCGCCGGAGGTGGACG AGGCCGCGCTGCGAGCATTCGTGCTGGAGAAGCGCTTCTGGATCTACACCAAGCTGGCCG AGAAGGACCGCTTGCAGCGCCAGGTTCCGCGCAAGGAATTCGTCGGAGGCGAGGGATTCT TGTATCTCGGCCGCAGCCATCGGCTGAAGGTGGTCGATGAACAGAATGTGCCACTGAAGT TGAATGGAGGCCGCTTTTGTCTGCGCCGTGACGCCCTACCCGCCGCGCGCGAGCATTTCA TCCGCTGGTACGGCGAGCGTGCCAAGGCCTGGCTTTCGGGGCGTGTAGCTGACTACCAGT CGCGAATGGAGGTGACGCCTGCCGGCGTCAAGGTGCAGGACCTTGGATATCGCTGGGGTT CGTGTGGCAAGGGCGACTGGCTGTACTTCCACTGGAAGGCAATCCTGCTGCCGGCGCGCA TCGCTGAGTATGTCGTGGTGCATGAGATTGCCCATCTGCATGAGCCGCACCACACGCCTG CGTTCTGGCTTCGAGTGGAGCGTGCCATGCCGGACTATGCGCAACGCAAGGCCTGGCTGG CCGAGCATGGAATCGATGTTGAAGGAATCTAAAGAACGATGGCTGACTATTTCACCAGTG ACTACTTCAAGCTGCTGAACAAGTGGAAGGGGCAGAAGCGTGACGAGTCCAACCCCGAGC AGAACCGCGCTTATGAAGATCTGAAGAAGGCCTACGAGGTGACGGAGGCGTGGGCGGACA AGGTTAAGGCCGAGTTGTTCCCTGTCGGGCGCGTCGAGATTCGTAAGCGCCCGACCAACC AGGGCAACAACTTTGCCAGCTACAACTGGGCCAAAATCTACCCTTCATCTGAGGCGCCGA AAGAGTTGGCTTACACAGTTGGCATCGGCGCCGATGACGGCTTCGTAGTCAAGATCGATA CCGTTGGGCTCGACGAATTGGACGCGACGAGAAAGGCCTAT

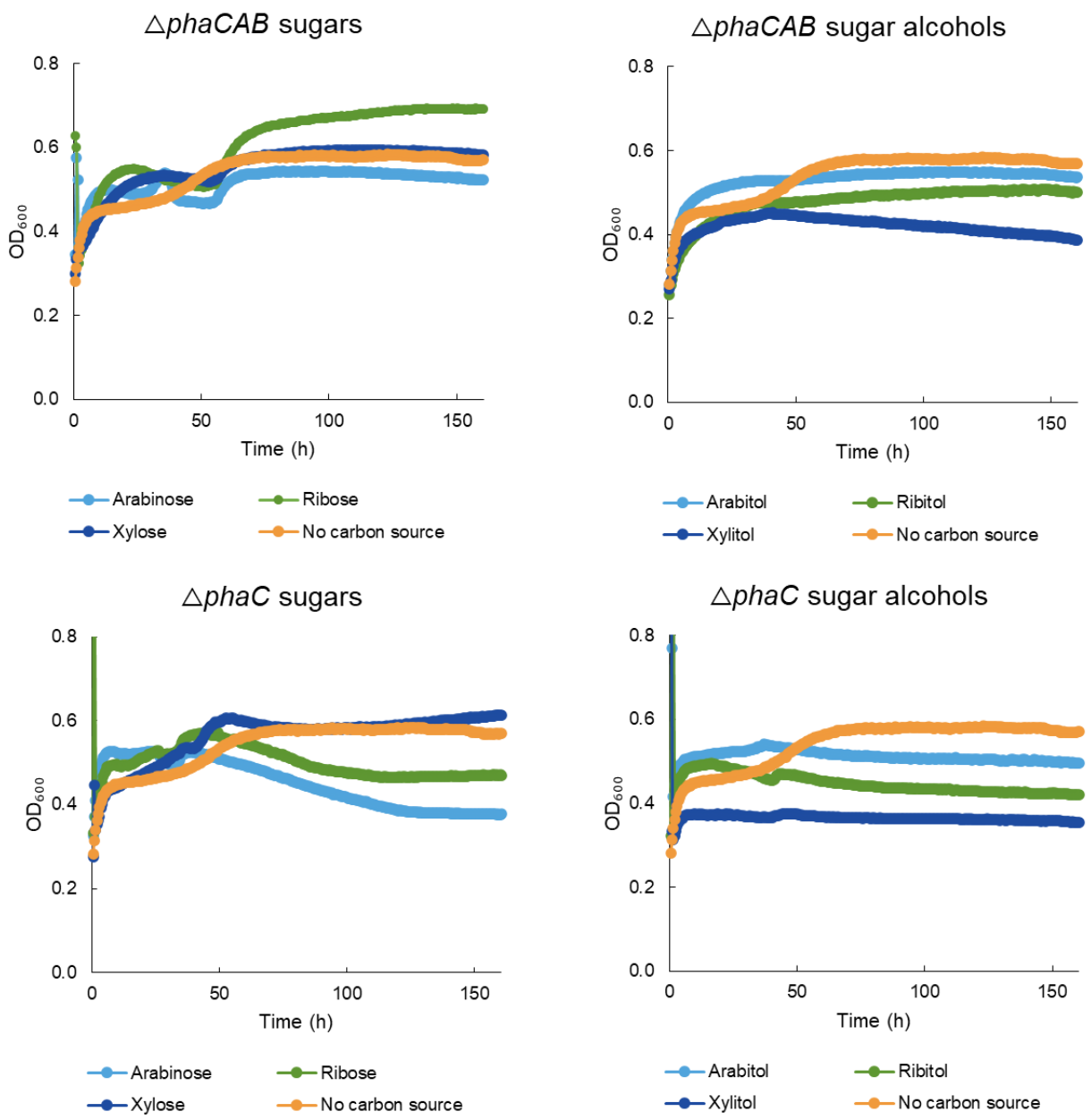

Figure S1. The growth of *C. necator* strains △*phaCAB* and △*phaC* on different sugars and sugar alcohols (100 mM). Precultures were grown in TSB. Cells were cultivated in 96-well plate at an initial OD_{600} of 0.05 in 130 µl of AUT media supplemented with the carbon sources. The cultures were topped with 50 µl of mineral oil to avoid evaporation. The negative control was cultivated in AUT media without any carbon source. The 96-well plate was incubated at 30°C using a double shake orbital at 282 rpm. All conditions had three replicates.

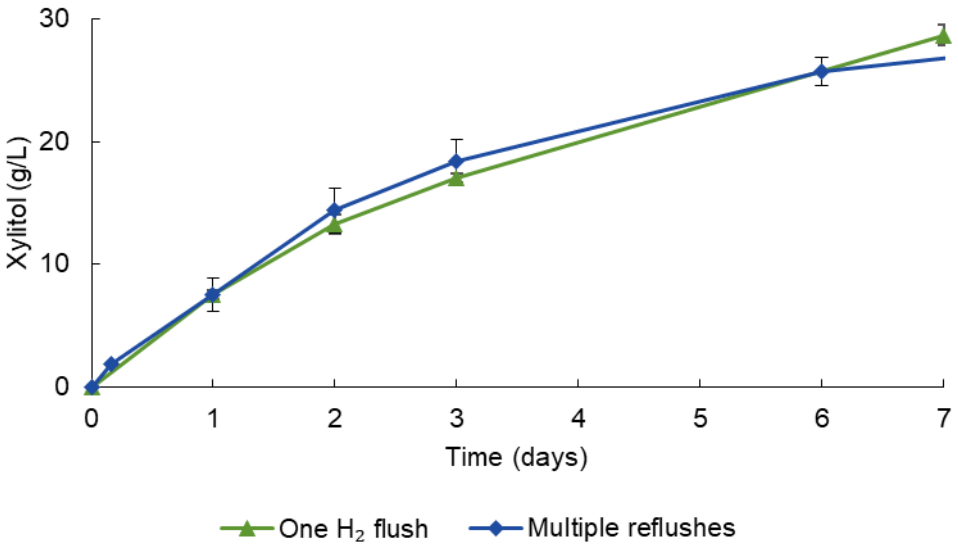

Figure S2. Comparison of bioconversion with a single H_2 flush at the start and H_2 flush after every sampling. The initial concentration of D-xylose was 34 g/L (one H_2 flush) and 30 g/L (multiple reflushes) in 100 mM sodium phosphate buffer (pH 7). The cell concentrations were OD_{600} of 13 (one H_2 flush) and OD_{600} of 17 (multiple reflushes).

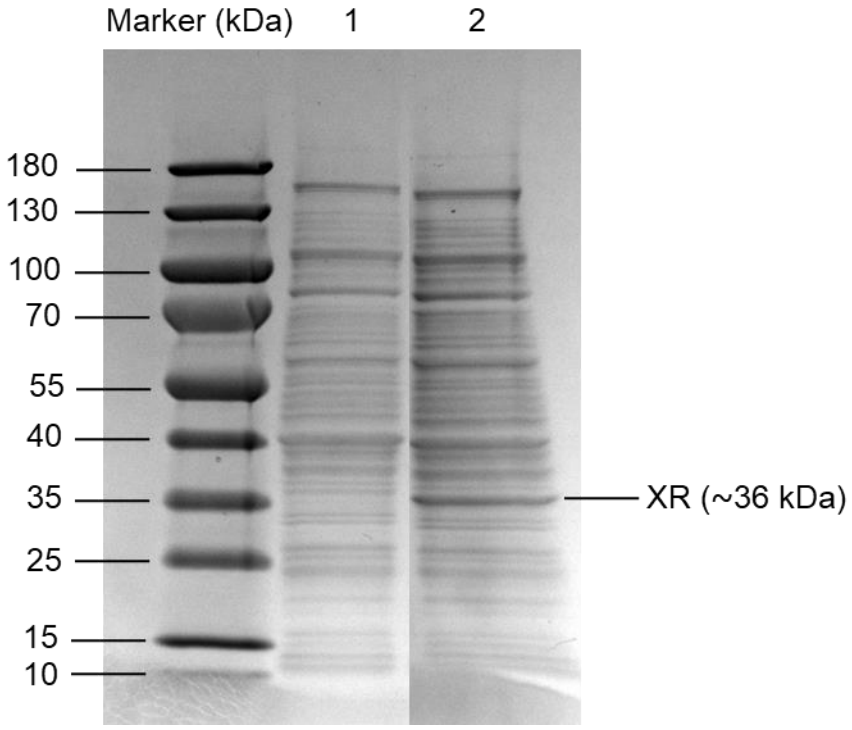

Figure S3. SDS-PAGE analysis of soluble extracts by *C. necator* H16 strains. Lane 1, wild type *C. necator* H16. Lane 2, △*phaCAB*_xr (△*phaCAB* with XRsti under Pj5 promoter).

Full calculations

Hydrogen consumption

The ideal gas law was used as a starting point for most of the calculations:

$$pV = nRT$$

Where p is the pressure (1 bar), V is the gas volume (L), n is the amount of gas (mol), R is the gas constant (0.08314 L bar K^{-1} mol^{-1}), and T is the temperature (298.15 K).

The total volume of the serum bottle was 50 mL, with an initial liquid volume of 5 mL. Consequently, the volume of the gas in the bottle was 45 mL, and no overpressure was applied. The initial hydrogen amount in the serum bottles can be calculated:

$$n_{H_2\ \mathrm{initial}} = \frac{pV}{RT} = \frac{1\ \mathrm{bar} \times 0.045\ \mathrm{L}}{0.083144\ \mathrm{L\ bar\ mol^{-1} K^{-1}} \times 298.15\ \mathrm{K}} = 1.815\ \mathrm{mmol}$$

When H_2 is consumed, only the pressure and the amount of hydrogen in the bottle change, as the gas volume is determined by the fixed volume of the bottle. However, when air is aspirated into the under-pressurized bottle, the volume of aspirated air is equal to the amount of hydrogen consumed. Consequently, the amount of hydrogen consumed can be estimated from the volume of air required to restore the pressure to atmospheric conditions. Additionally, sampling contributed to the under-pressure and must be accounted for:

$$V_{\mathrm{sampling}} = 0.2\ \mathrm{mL} \times 4 = 0.8\ \mathrm{mL}$$

The average aspirated volume into the serum flasks was 30 mL. The consumed H_2 volume was calculated by subtracting the sampling volume:

$$V_{H_2\ \mathrm{consumed}} = 30\ \mathrm{mL} - 0.8\ \mathrm{mL} = 29.2\ \mathrm{mL}$$

The amount of hydrogen consumed per bottle:

$$n_{H_2\ \mathrm{consumed}} = \frac{pV}{RT} = \frac{1\ \mathrm{bar} \times 0.0292\ \mathrm{L}}{0.083144\ \mathrm{L\ bar\ mol^{-1} K^{-1}} \times 298.15\ \mathrm{K}} = 1.178\ \mathrm{mmol}$$

The proportion of the initial H_2 consumed per bottle is therefore:

$$\text{Proportion of initial } H_2 \text{ consumed} = \frac{n_{H_2\ \text{consumed}}}{n_{H_2\ \text{initial}}} \times 100\% = \frac{1.178\text{mmol}}{1.815\ \text{mmol}} \times 100\% = 65\%$$

Xylitol production

The amount of xylitol in the final samples was 46 g/L, which corresponds to 302 mM of xylitol. The final volume in the bottles was around 4.2 mL, considering that 0.8 mL was removed for sampling. Therefore, the final amount of xylitol in the serum bottles was:

$$n_{\text{xylitol final}} = 0.302\ \text{M} \times 4.2\ \text{mL} = 1.268\ \text{mmol}$$

Considering the xylitol in the samples, the total xylitol concentration produced was:

$$n_{\text{xylitol total}} = n_{\text{xylitol final}} + n_{\text{xylitol in samples}} \approx 1.3\ \text{mmol}$$

Since some xylitol was produced without the presence of H_2, this amount must be subtracted from the total to account for xylitol production with H_2:

$$n_{\text{xylitol produced with } H_2} = n_{\text{xylitol total}} - n_{\text{xylitol produced without } H_2} = 1.3\ \text{mmol} - 0.2\ \text{mmol} = 1.1\ \text{mmol}$$

Amount of H_2 used for xylitol production from

Since one mole of H_2 is needed to reduce one mole of xylose, the amount of H_2 used for xylitol production is 1.1 mmol. The proportion of H_2 used for xylitol production is:

$$\text{Proportion of } H_2 \text{ used for xylitol production} = \frac{n_{H_2 \text{used for xylitol production}}}{n_{H_2 \text{consumed}}} \times 100\%$$
$$= \frac{1.1\ \text{mmol}}{1.178\ \text{mmol}} \times 100\% = 93\ \%$$

Error considerations

These calculations are estimates, and several factors may contribute to errors:

- The aspirated volume was measured using a 50 mL syringe, which lacks a fine-scale resolution.
- Sampling was performed with a 1 mL syringe, which also has limited scale resolution.
- Inaccurate sampling volumes can affect the total calculated amount of xylitol produced.
- The xylitol amount in samples is an average from multiple conversions.
- The xylitol amount which was produced without H_2 is also an average from multiple conversions.